# Modelling and simulation of turbulence subject to system rotation

by

Olof Grundestam

March 2006 Technical Reports from Royal Institute of Technology Department of Mechanics SE-100 44 Stockholm, Sweden Typsatt i  $\mathcal{A}_{\mathcal{M}}\mathcal{S}$ -IATEX.

Akademisk avhandling som med tillstånd av Kungliga Tekniska Högskolan i Stockholm framlägges till offentlig granskning för avläggande av teknologie doktorsexamen fredagen den 17:e mars 2006 kl. 10.15 i sal F2, Kungliga Tekniska Högskolan, Valhallavägen 79, Stockholm.

©Olof Grundestam 2006 Universitetsservice US-AB, Stockholm 2006

#### Simulation and modelling of turbulence subject to system rotation

Olof Grundestam Department of Mechanics, Royal Institute of Technology SE-100 44 Stockholm, Sweden.

#### Abstract

Simulation and modelling of turbulent flows under influence of streamline curvature and system rotation have been considered. Direct numerical simulations have been performed for fully developed rotating turbulent channel flow using a pseudo-spectral code. The rotation numbers considered are larger than unity. For the range of rotation numbers studied, an increase in rotation number has a damping effect on the turbulence. DNS-data obtained from previous simulations are used to perform a priori tests of different pressure-strain and dissipation rate models. Furthermore, the ideal behaviour of the coefficients of different model formulations is investigated. The main part of the modelling is focused on explicit algebraic Reynolds stress models (EARSMs). An EARSM based on a pressure strain rate model including terms that are tensorially nonlinear in the mean velocity gradients is proposed. The new model is tested for a number of flows including a high-lift aeronautics application. The linear extensions are demonstrated to have a significant effect on the predictions. Representation techniques for EARSMs based on incomplete sets of basis tensors are also considered. It is shown that a least-squares approach is favourable compared to the Galerkin method. The corresponding optimality aspects are considered and it is deduced that Galerkin based EARSMs are not optimal in a more strict sense. EARSMs derived with the least-squares method are, on the other hand, optimal in the sense that the error of the underlying implicit relation is minimized. It is further demonstrated that the predictions of the least-squares EARSMs are in significantly better agreement with the corresponding complete EARSMs when tested for fully developed rotating turbulent pipe flow.

**Descriptors:** Direct numerical simulations, least-squares method, turbulence model, nonlinear modelling, system rotation, streamline curvature, high-lift aerodynamics.

# **Preface**

This thesis is based on and contains the following papers:

- **Paper 1.** OLOF GRUNDESTAM, STEFAN WALLIN & ARNE V. JOHANSSON 2005 Techniques for deriving explicit algebraic Reynolds stress models based on incomplete sets of basis tensors and predictions of fully developed rotating pipe flow *Phys. Fluids*, 2005, **17**.
- **Paper 2.** OLOF GRUNDESTAM, STEFAN WALLIN & ARNE V. JOHANSSON 2004 An explicit algebraic Reynolds stress model based on a nonlinear pressure strain rate model. *Int. J. Heat Fluid Flow*, 2005, **26**.
- **Paper 3.** OLOF GRUNDESTAM, STEFAN WALLIN & ARNE V. JOHANSSON 2006 Observations on the predictions of fully developed rotating pipe flow using differential and explicit algebraic Reynolds stress models. *Euro. J. Mech. B/Fluids*, 2006, **25**.
- Paper 4. OLOF GRUNDESTAM, STEFAN WALLIN, PETER ELIASSON & ARNE V. JOHANSSON 2005 Application of EARSM turbulence models to high-lift aerodynamics applications. *Proc. of Engineering turbulence modelling and measurements 6 (ETMM-6)*, Sardinia, Italy.
- Paper 5. OLOF GRUNDESTAM, STEFAN WALLIN & ARNE V. JOHANSSON 2006 Direct numerical simulations of rotating channel flow. To be submitted.
- **Paper 6.** OLOF GRUNDESTAM, STEFAN WALLIN & ARNE V. JOHANSSON 2006 A priori evaluations and least-squares optimizations of turbulence models for fully developed rotating turbulent channel flow. *To be submitted.*

The papers are re-set in the present thesis format.

#### Division of work between authors

The work presented in this thesis has been done in collaboration with other researchers. No development of computational codes has been done except for the necessary maple programming needed to derive the algebraic expressions appearing in several of the papers. The numerical solver for one dimensional problems, featuring a MAPLE based user interface, that is used in papers 1-3, has been developed by Stefan Wallin (SW). The EDGE-code used in paper 4 is the general flow solver developed and administrated by the Swedish Defence Research Agency (FOI). Arne V. Johansson (AJ) has acted main supervisor throughtout the whole study and has contributed, in addition to what is stated below, with valuable discussions and comments.

Paper 1 is based on ideas of Olof Grundestam (OG) and Stefan Wallin (SW). The algebra, implementation and computations were carried out by OG.

The work of paper 2 were performed within the HiAer project, a European project, (Project Ref: G4RD-CT-2001-00448) and was the first investigation undertaken in the present study.

Paper 3 came as a natural extension of paper 2 and was performed in order to answer some of the questions inherited from the preceding study. The investigation were carried out by OG and were discussed with SW and AJ.

The work of paper 4 was performed in close collaboration with SW. OG implemented the EARSM proposed in paper 2 in the EDGE-code. Peter Eliasson (PE) at FOI performed the 3D computations and evaluated the corresponding data. PE also wrote the part of the paper concerning the 3D case.

The computations and evaluations of paper 5 were performed by OG using the pseudo-spectral code developed earlier at the mechanics department at KTH. AJ has contributed much to this paper in terms of discussions, reasoning and comments on the text.

The evaluations of paper 6 was performed by OG. The ideas have been developed together with SW.

The writing of all papers has mainly been done by OG. The contributions from all co-authors have, however, been invaluable.

# Contents

Preface	iv
Chapter 1. Introduction	1
Chapter 2. Basic equations	4
2.1. Navier-Stokes equations	4
2.2. Turbulence closures	6
2.2.1. Differential Reynolds stress models	7
2.2.2. Explicit algebraic Reynolds stress models	9
2.3. Generic test cases	12
Chapter 3. Formulation of EARSMs	14
3.1. Complete EARSMs	14
3.2. Incomplete EARSMs	15
3.2.1. Optimality	18
3.2.2. Singularities	20
3.3. Nonlinear modelling for EARSMs	21
Chapter 4. DNS of rotating channel flow	24
4.1. Least-squares optimizations of model parameters	28
Chapter 5. Conclusions and outlook	30
Chapter 6. Acknowledgement	32
Bibliography	33

# viii CONTENTS

Paper 1.	Techniques for deriving explicit algebraic Reynolds stress models based on incomplete sets of basis tensors and predictions of fully developed rotating pipe flow	39
Paper 2.	An explicit algebraic Reynolds stress model based on a nonlinear pressure strain rate model	67
Paper 3.	Observations on the predictions of fully developed rotating pipe flow using differential and explicit algebraic Reynolds stress models	95
Paper 4.	11	127
Paper 5.	Direct numerical simulations of rotating channel flow	143
Paper 6.	of turbulence models for fully developed rotating	165

#### CHAPTER 1

# Introduction

Fluid flow has fascinated and puzzled man through all times and still does. What probably began as a mere desire of being able to fly has gradually evolved to the search of insight and understanding of the most fundamental mechanisms of fluid flow. Today, we are indeed able to construct flying machines and man's knowledge in the field of fluid mechanics has greatly increased, but even though the governing Navier-Stokes equations are known and numerous experiments have been performed, the research in this area is more intense than ever.

From a physical point of view, all gases are composed of one or many species of atoms or molecules. These molecules move along straight trajectories in space until they are sufficiently close to one another to interact. These dynamics are governed by the Boltzmann equation which is an equation for the particle probability density in phase space. In between two "collisions", a gas molecule travels a distance referred to as the mean-free path. If the mean-free path is small enough compared to the characteristic length-scales of the problem, the particle system can be treated as a continuum or a fluid. In the continuum limit the first-order approximation of the Boltzmann equation equals the Navier-Stokes equations, the governing equations of fluid flow. From this perspective the Navier-Stokes equations provide a mathematical approximation of the physical reality, valid only in the continuum limit. It should be pointed out that the corresponding dynamics governing liquids are far more complicated than for gases. In the continuum limit, however, liquid flow is also governed by the Navier-Stokes equations. For the remaining part of the present work the assumption of a continuum is always applied.

Although the equations governing the flow are known, the complexity of the flow makes it impossible to find analytical solutions for most cases of interest. Experiments can of course be performed to study a particular flow case but with the measurement techniques available today it may be difficult to extract all information of interest. It is therefore necessary to use numerical methods to solve the Navier-Stokes equations. Solutions that are exact (to the order of the numerical method used) can be obtained in a direct numerical simulation (DNS) in which the governing equations are solved directly and all details of the flow are given. But due to the wide range of scales of the flow, the turbulence, the computational effort rapidly becomes extreme. DNS is therefore applicable only in a number of generic flows where the range of scales is relatively restricted. From this perspective experiments are attractive since they can,

#### 2 1. INTRODUCTION

at least in principle, be performed for any flow case. However, in engineering design processes in which DNS is not applicable due to computational expenses and experiments provide a time consuming and costly tool since every design of interest has to be physically manufactured, less demanding (and therefore approximative) computationally based procedures are needed.

An approximative method useful for engineering types of problems is based on averaging the Navier-Stokes equations. With this approach, a set of equations commonly referred to as the Reynolds averaged Navier-Stokes (RANS) equations are solved. The numerical cost of a RANS-computation is far less than for a DNS since only the mean flow has to be resolved. Hence, computations involving large objects subject to high free-stream velocities, such as airplanes, can be performed. The drawback with this procedure is that the equations governing the mean flow depend on a set of unknown quantities, the Reynolds stresses, which correspond to the extra transport of momentum due to the turbulence. A new equation for the Reynolds stresses can be derived but it turns out that this equation depends on new unknown quantities and the equations for these do in turn depend on other unknown quantities and so forth. This problem is due to the nonlinearity of the Navier-Stokes equations and is referred to as the closure problem (of turbulence). In order to close the system of equations, modelling (approximations) has to be introduced at some level. This is the nature behind the term "turbulence modelling". Another approach that is gaining in interest is large eddy simulations (LES) in which the large eddies of the flow are resolved. This is computationally more cumbersome than the RANS-procedure but considerably more physics are included. In the present study no LES computations have been performed.

A typical RANS-turbulence closure incorporates, in addition to the mean velocity equations, a constitutive relation connecting the turbulent stresses with the mean velocity gradients and a two-equation platform which normally consists of one equation for the turbulence kinetic energy and one equation for a quantity of different dimension, such as the dissipation rate. Alternatively, a full transport equation of the turbulent stresses in combination with a length-scale determining equation can be used. Regardless of which approach is chosen, the turbulence model relies on a number of parameters that need to be calibrated. This is usually done by considering a generic type of flow and tuning the parameters in such a way that the predictions of the RANS-closure correspond to the observations of an experiment or a DNS. From this point of view a DNS is particularly useful since all flow quantities and correlations are available. Furthermore, by using DNS-data the physical correctness of the individual components of a turbulence model can be investigated in so called a priori tests.

The field of applications for fluid mechanics is vast and includes everything from meteorology and aeronautical vehicle design to biophysics phenomena such as blood flow in the brain. Hence, generality is a very important aspect of turbulence modelling. In order to be able to give a RANS-closure any significance as a predictive tool, the behaviour in a large number of flows must be assessed. Generality is normally easier to achieve with models that incorporate as much flow physics as possible. This on the other hand, means an increased computational effort.

In the present work different aspects of turbulence modelling are discussed. The emphasis is on the constitutive relation for which different modelling and approximation techniques are investigated. The assessment is focused on generic geometrically simple flow cases with one exception, an aeronautics high-lift geometry that serves as an illustration of an important engineering application. The study also incorporates a DNS of turbulent channel flow subject to rapid system rotation.

#### CHAPTER 2

# Basic equations

# 2.1. Navier-Stokes equations

All details of a fluid flow are given by the governing Navier-Stokes equations which can be derived from Newton's second law by condsidering a fluid element and the stresses acting upon it. The total stress is composed of the two parts, i) the pressure which exerts a force normal to the surface of the fluid element and ii) the viscous forces from the surrounding elements. For a fluid such as air or water, the viscous forces are directly proportional to the rate of deformation, the strain rate, of the fluid with a proportionality coefficient equal to the viscosity. Fluids which have this relation between stress and strain rate are commonly denoted Newtonian fluids. Only Newtonian fluids are considered in the present study. In what follows we shall also assume incompressibility meaning that the density is constant. The incompressibilty assumption is justified at low mach number flows, i.e. when the velocity is low compared to the speed of sound and for small temperarture variations. Under these assumptions the Navier-Stokes equations take the form

$$\frac{\partial u_i}{\partial x_i} = 0 (2.1)$$

$$\frac{\partial u_i}{\partial x_i} = 0$$

$$\frac{\partial u_i}{\partial t} + u_j \frac{\partial u_i}{\partial x_j} = -\frac{1}{\rho} \frac{\partial p}{\partial x_i} + \frac{\partial}{\partial x_j} (2\nu s_{ij})$$
(2.1)

in Cartesian tensor notation in an inertial frame of reference.  $\rho$  is the density and  $\nu$  the kinematic viscosity of the fluid. (2.1) is the continuity condition (conservation of mass) for an incompressible fluid which dictates that the velocity field is divergence free. (2.2) governs the momentum.  $s_{ij}$  is the strain rate tensor and is given by

$$s_{ij} = \frac{1}{2} \left( \frac{\partial u_i}{\partial x_j} + \frac{\partial u_j}{\partial x_i} \right) \tag{2.3}$$

 $u_i$  and p are the instantaneous velocity components and pressure. Note that the strain rate tensor is symmetric and traceless.

Equation (2.1) and (2.2) can be solved directly in a so called direct numerical simulation (DNS). In order to have a physically accurate solution, the smallest scales of the flow must to be resolved. By smallest scales are meant the smallest intervals in space and time that are important for the flow. A

measure of the range of scales is the Reynolds number which is defined as

$$Re = \frac{UL}{\nu} \tag{2.4}$$

where U and L are characteristic velocity and length scales. Hence the computational effort for increasing Reynolds numbers increases rapidly. Therefore, DNS can only be used to study relatively simple geometries at restricted Reynolds numbers. This limits DNS to be used as mainly a research tool for fundamental aspects of turbulence and for evaluating and calibrating turbulence models. It should be pointed out that different Reynolds numbers can be defined for the same flow case depending on what scales are chosen as reference.

At higher Reynolds numbers, in e.g. engineering type of applications, statistical methods must be used. A widely used approach is based on averaging the Navier-Stokes equations (2.2) by decomposing the velocity and pressure fields into mean and fluctuating parts according to  $u_i = U_i + u_i'$  and p = P + p'.  $P = \overline{p}$  and  $U_i = \overline{u_i}$  are the mean parts where a bar means averaging.  $u_i'$  and p' are the fluctuating parts for which  $\overline{u_i'} = 0$  and  $\overline{p'} = 0$ . In this way a set of equations referred to as the Reynolds averaged Navier-Stokes (RANS) equations are obtained. They read

$$\frac{\partial U_i}{\partial x_i} = 0 (2.5)$$

$$\frac{\partial U_i}{\partial t} + U_j \frac{\partial U_i}{\partial x_j} = -\frac{1}{\rho} \frac{\partial P}{\partial x_i} + \frac{\partial}{\partial x_j} (2\nu S_{ij} - \overline{u_i' u_j'})$$
 (2.6)

where the mean strain rate tensor, defined in analogy with (2.3), has the components

$$S_{ij} = \frac{1}{2} \left( \frac{\partial U_i}{\partial x_j} + \frac{\partial U_j}{\partial x_i} \right) \tag{2.7}$$

in Cartesian tensor notation. While (2.6) is an equation for the mean velocity, the dependency on the turbulence enters through  $\overline{u_i'u_j'}$ , the Reynolds stress, which is the extra flux of momentum due to the turbulent fluctuations. Hence, in order to be able to solve (2.6),  $\overline{u_i'u_j'}$  must be evaluated. The natural way to proceed is to investigate the transport equation for the Reynolds stresses which can be derived from the Navier-Stokes equations and (in an inertial frame of reference) reads

$$\frac{D\overline{u_i'u_j'}}{Dt} = \mathcal{P}_{ij} - \varepsilon_{ij} + \Pi_{ij} + \mathcal{D}_{ij}$$
(2.8)

where  $D/Dt = \partial/\partial t + U_j\partial/\partial x_j$ . The terms on the right-hand side represent production, dissipation, pressure-strain and diffusion respectively. The exact

expressions for these are given by

$$\mathcal{P}_{ij} = -\overline{u'_i u'_m} \frac{\partial U_j}{\partial x_m} - \overline{u'_j u'_m} \frac{\partial U_i}{\partial x_m}$$

$$\varepsilon_{ij} = 2\nu \overline{u'_{i,m} u'_{j,m}}$$
(2.9)

$$\varepsilon_{ij} = 2\nu \overline{u'_{i,m} u'_{j,m}} \tag{2.10}$$

$$\Pi_{ij} = \frac{2}{\rho} \overline{p's'_{ij}} \tag{2.11}$$

$$\mathcal{D}_{ij} = -\frac{\partial}{\partial x_m} \left( J_{ijm} - \nu \frac{\partial \overline{u_i' u_j'}}{\partial x_m} \right)$$
 (2.12)

where a comma is used to denote differentiation and

$$J_{ijm} = \overline{u_i' u_j' u_m'} + \frac{1}{\rho} (\overline{u_j' p'} \delta_{im} + \overline{u_i' p'} \delta_{jm})$$
 (2.13)

The production tensor is the direct interaction between the mean flow and the turbulence and can be interpreted as the energy transfer rate from the mean flow to the fluctuations. In some rare cases this term can have the opposite effect and transfer energy from the turbulence to the mean flow. The pressure-strain rate tensor is associated with intercomponent energy transfer among the Reynolds stress components since it is traceless and hence have no direct effect on the total turbulence kinetic energy,  $K = \overline{u_i u_i}/2$  (summation convention assumed). The dissipation represents the viscous dissipation into heat. The diffusion terms includes both diffusion due to viscous stresses and fluctuations in velocity and pressure. Obviously only the production can be expressed in terms of quantities that are solved for, the Reynolds stress and the mean velocity gradients. The other terms depend on unknown correlations. Furthermore, the transport equations for the these correlations are dependent on new unknown correlations. This is the well known closure problem of turbulence caused by the nonlinearity of the Navier-Stokes equation. The solution to this dilemma is to introduce modelling at some level in order to close the system of equations. The branch of turbulence modelling is hence concerned with the closure problem and the necessary approximations. It should be pointed out, however, that a turbulence model does not necessarily involve (2.8) as discussed below. Since the first efforts were made by Boussinesq (1877) the list of proposed turbulence closures have grown long, and it is still growing.

#### 2.2. Turbulence closures

A great number of RANS turbulence models can be found in the litterature. These can vary a great deal regarding underlying modelling assumptions as well as complexity. In the present work, mainly two different types of models are discussed, differential Reynolds stress models and explicit algebraic Reynolds stress models. Brief descriptions of the essentials of these and related approaches are given below.

#### 2.2.1. Differential Reynolds stress models

Turbulence models based on the transport equations for the Reynolds stresses are usually called Reynolds stress transport (RST) models or differential Reynolds stress models (DRSM). From a mathematical point of view, this family of models seems as the natural choice for modelling the Reynolds stress in RANS-closures since no ad-hoc assumptions other than those necessary for the modelling of the terms in these equations have to be made. In this approach the full transport equation of the Reynolds stresses (2.8) is solved in combination with an equation for an auxiliary quantity. This means that seven equations must be solved for the general three-dimensional case in addition to the mean flow equations since the Reynolds stress tensor is symmetric. Alternatively, the transport equation for the Reynolds stress anisotropy tensor,

$$a_{ij} = \frac{\overline{u_i u_j}}{K} - \frac{2}{3} \delta_{ij} \tag{2.14}$$

which is symmetric and traceless, can be considered.  $K = \overline{u_i u_i}/2$  is the turbulence kinetic energy and the corresponding transport equation can be obtained by taking half the trace of (2.8)

$$\frac{DK}{Dt} = \mathcal{P} - \varepsilon + \mathcal{D} \tag{2.15}$$

where the terms on the right-hand side terms denote half the trace of the corresponding terms of (2.8). Note that the pressure-strain rate tensor is traceless,  $\Pi_{ii} = 0$ . The transport equation for  $a_{ij}$  can then be derived by combining (2.8) and (2.15). This yields

$$K\frac{Da_{ij}}{Dt} = -\left(a_{ij} + \frac{2}{3}\delta_{ij}\right)(\mathcal{P} - \varepsilon) + \mathcal{P}_{ij} - \varepsilon_{ij} + \Pi_{ij} + \mathcal{D}_{ij}^{(\mathbf{a})}$$
(2.16)

in an inertial frame.  $\mathcal{D}_{ij}^{(\mathbf{a})} = \mathcal{D}_{ij}/K - \overline{u_i u_j} \mathcal{D}/K^2$  is the diffusion of the Reynolds stress anisotropy.

In order to be able to determine the turbulent stresses, (2.16) is complemented with a two-equation platform that normally incorporates the transport equation for the turbulence kinetic energy (2.15) and an auxiliary quantity of different dimension. For the latter purpose, the perhaps most natural choice is the dissipation rate of the turbulence kinetic energy,  $\varepsilon = \varepsilon_{ii}/2$ . However, other quantities, formed from K and  $\varepsilon$ , can sometimes be preferred. The modelled transport equation for an auxiliary quantity on the form  $Z = K^m \varepsilon^n$ , can be schematically written as

$$\frac{DZ}{Dt} = \frac{Z}{K} (C_{Z1} \mathcal{P} - C_{Z2} \varepsilon) + \mathcal{D}^{(Z)}$$
(2.17)

where  $C_{Z1}$  and  $C_{Z1}$  are model parameters. In addition, cross diffusion terms that occur naturally in the transformation  $Z = Z(K, \varepsilon)$  can be incorporated.

It should be noted that the alternative to using a turbulence closure consisting of (2.16), (2.15) and (2.17), would be to use (2.8) in combination with (2.17). These approaches are in principle equivalent but due to differences

in the boundary conditions and the choice of numerical method, one set of equations might be preferred over the other.

Since all terms of (2.8) (or (2.16)) are included, the different physical interactions of the components with each other and the mean flow are considered. Effects of streamline curvature and system rotation which can be strong in many applications are included in a natural way in this type of model. Hence, the predictions of a DRSM can be expected to be more accurate in a larger number of flows than those of simpler turbulence models.

There have been numerous suggestion of how to model the different terms of the transport equation for  $\overline{u_i'u_j'}$ . The dissipation rate tensor is quite often modelled using an isotropic model as  $\varepsilon_{ij} = 2\varepsilon\delta_{ij}/3$  where  $\varepsilon$  is determined from the length and velocity scale determining equations. A dissipation rate model that is nonlinear in the Reynolds stress anisotropy tensor has been proposed by Sjögren & Johansson (2000). Another interesting modelling approach has recently been suggested by Perot & Natu (2004). They develop a dissipation rate tensor model that is exact in the limit of very strong inhomogeneity. Since the modelling of the dissipation and the slow pressure strain rate tensors is done in the same fashion, the models are sometimes lumped together, see for instance Gatski & Speziale (1993). An often used diffusion model has been proposed by Daly & Harlow (1970). This is on the form

$$\mathcal{D}_{ij} = \frac{\partial}{\partial x_l} \left[ \left( \nu \delta_{lk} + c_s \frac{K}{\varepsilon} \overline{u_l u_k} \right) \frac{\partial \overline{u_i u_j}}{\partial x_k} \right]$$
 (2.18)

where  $c_s$  is a model parameter. The corresponding expression can also be used to model the diffusion of the auxiliary quantity.

The term that provides the greatest challenge for the turbulence modeller is the pressure-strain rate tensor. This term is traceless and represents intercomponent energy redistribution. It is associated with non-local interactions and is therefore complicated to accurately predict in single-point closures. The modelling of the pressure-strain rate correlation is normally based on the formal solution of the Poisson equation for the fluctuating pressure. The character of the inhomogeneous terms naturally divides the solution into three parts: the rapid and slow parts and the Stokes term. The rapid part depends explicitly on the mean velocity gradient and therefore responds directly to changes in the mean flow whereas the slow part depends only on the fluctuating velocities, see Hallbäck *et al.* (1996). The modelled pressure-strain rate tensor can, in analogy with this, be divided into three parts: slow and rapid pressure strain,  $\Pi_{ij}^{(s)}$  and  $\Pi_{ij}^{(r)}$  respectively, and a pressure reflection part emanating from the Stokes pressure which might become significant close to the wall.

The most general quasi-linear model for the total pressure strain rate tensor lumped together with the dissipation rate anisotropy tensor is given by

$$\frac{\mathbf{\Pi}}{\varepsilon} - \mathbf{e} = -\frac{1}{2} \left( C_1^0 + C_1^1 \frac{\mathcal{P}}{\varepsilon} \right) \mathbf{a} + C_2 \tau \mathbf{S} 
+ \frac{C_3 \tau}{2} (\mathbf{a} \mathbf{S} + \mathbf{S} \mathbf{a} - \frac{2}{3} \{ \mathbf{a} \mathbf{S} \} \mathbf{I}) - \frac{C_4 \tau}{2} (\mathbf{a} \mathbf{\Omega} - \mathbf{\Omega} \mathbf{a})$$
(2.19)

where  $e_{ij} = \varepsilon_{ij}/\varepsilon - 2\delta_{ij}/3$ . In (2.19) a bold face notation has been used where, for instance, **S** is the strain rate tensor with components  $S_{ij}$ .  $\Omega$  is the mean rotation rate tensor and is given by the antisymmetric part of the mean velocity gradient tensor. Whereas **S** preserves its form when transformed to a rotating frame of reference, the transformation of  $\Omega$  gives rise to an extra term including the system rotation rate vector,  $\omega^{(s)}$ . The obtained tensor is commonly denoted the absolute rotation rate tensor and has components given by

$$\Omega_{ij} = \frac{1}{2} \left( \frac{\partial U_i}{\partial x_j} - \frac{\partial U_j}{\partial x_j} \right) - \epsilon_{ijk} \omega_k^{(s)}$$
(2.20)

In a nonrotating frame of reference the contribution due to system rotation is, of course, zero.

The model (2.19) is quasilinear in the Reynolds stress anisotropy since  $\mathcal{P}/\varepsilon = -\tau a_{ij}S_{ij}$  where  $\tau = K/\varepsilon$  is the turbulence time-scale. Many proposed pressure-strain rate models can be written on the form (2.19), see for instance Launder et al. (1975) (LRR-model). Speziale et al. (1991) included a term quadratic in their model, the SSG-model. This model also exists in a linearized version, the L-SSG model which can be written on the same form as (2.19), see Gatski & Speziale (1993). Johansson & Hallbäck (1994) derived the expression for the most general model for the rapid pressure strain. The tensorial expression for their model was obtained by studying the symmetries of the formal expression for the rapid pressure strain. This gave a model including terms nonlinear in the Reynolds stress anisotropy tensor. The model by Johansson & Hallbäck (1994) was incorporated in a DRSM by Sjögren & Johansson (2000).

Compared to other simpler turbulence models, the computational effort for a DRSM is significantly larger and the numerical behaviour in terms of, e.g., robustness can be troublesome. Despite this, turbulence closures based on the transport equations of the Reynolds stresses are preferred in more complex flows since effects of streamline curvature effects, diffusion and intercomponent energy transfer are included in a natural way.

#### 2.2.2. Explicit algebraic Reynolds stress models

An explicit algebraic Reynolds stress model (EARSM) is derived from the transport equation of the Reynolds stress anisotropy (2.16) and consists of an explicit relation between the Reynolds stress anisotropy and the mean velocity gradients. By basing the model formulation on the full transport equation of  $a_{ij}$ , good predictions can be expected in a wide range of flows, but since an EARSM is explicit, no extra transport equation for  $a_{ij}$  needs to be solved. The

computational effort is therefore significantly smaller than that of a DRSM. This family of models came as a natural extension of the weak-equilibium assumption proposed by Rodi (1976). In the weak-equilibrium limit the Reynolds stress anisotropy varies slowly in time and space implying that the advection and diffusion of the anisotropy become small and can be neglected. The transport equation for the anisotropy hence reduces to an algebraic equation for  $a_{ij}$ 

$$\left(a_{ij} + \frac{2}{3}\delta_{ij}\right)\left(\frac{\mathcal{P}}{\varepsilon} - 1\right) = \frac{1}{\varepsilon}(\mathcal{P}_{ij} - \varepsilon_{ij} + \Pi_{ij})$$
 (2.21)

This implicit relation in combination with a two-equation platform may in principle be used for determining  $\overline{u_i'u_j'}$  for any kind of pressure-strain and dissipation rate models. A model of this kind is commonly referred to as an algebraic Reynolds stress model (ARSM). An EARSM is obtained when the solution of (2.21) is written on explicit form. This was first done by Pope (1975) who found a tensorial solution to (2.21) in terms of the velocity gradients for two dimensional mean flows. In the work of Pope (1975) the scalar nonlinearity due to  $\mathcal{P}/\varepsilon = -\tau a_{ij}S_{ij}$  was avoided by treating  $\mathcal{P}/\varepsilon$  as an extra unknown. The explicit relation is usually given as a representation in terms of a set of basis tensors  $\{T_{ij}^{(k)}\}$  as

$$a_{ij} = \beta_k T_{ij}^{(k)} \tag{2.22}$$

where the summation convention is applied. Basis tensors often used for EARSM representation are

$$\begin{array}{lll} \mathbf{T}^{(1)} = \mathbf{S} & \mathbf{T}^{(2)} = \mathbf{S}^2 - \frac{1}{3}II_{\mathbf{S}}\mathbf{I} \\ \mathbf{T}^{(3)} = \Omega^2 - \frac{1}{3}II_{\Omega}\mathbf{I} & \mathbf{T}^{(4)} = \mathbf{S}\Omega - \Omega\mathbf{S} \\ \mathbf{T}^{(5)} = \mathbf{S}^2\Omega - \Omega\mathbf{S}^2 & \mathbf{T}^{(6)} = \mathbf{S}\Omega^2 + \Omega^2\mathbf{S} - \frac{2}{3}IV\mathbf{I} \\ \mathbf{T}^{(7)} = \mathbf{S}^2\Omega^2 + \Omega^2\mathbf{S}^2 - \frac{2}{3}V\mathbf{I} & \mathbf{T}^{(8)} = \mathbf{S}\Omega\mathbf{S}^2 - \mathbf{S}^2\Omega\mathbf{S} \\ \mathbf{T}^{(9)} = \Omega\mathbf{S}\Omega^2 - \Omega^2\mathbf{S}\Omega & \mathbf{T}^{(10)} = \Omega\mathbf{S}^2\Omega^2 - \Omega^2\mathbf{S}^2\Omega \end{array}$$
(2.23)

in which a bold-face notation has been used and normalization with the turbulence time-scale  $\tau$  has been assumed, i.e.  $S_{ij} \to \tau S_{ij}$  and  $\Omega_{ij} \to \tau \Omega_{ij}$ . Five independet invariants may be formed from the mean velocity gradients for the most general three-dimensional mean flows. These are

$$II_{\mathbf{S}} = \{\mathbf{S}^2\} \quad II_{\mathbf{\Omega}} = \{\mathbf{\Omega}^2\} \quad III_{\mathbf{S}} = \{\mathbf{S}^3\}$$

$$IV = \{\mathbf{S}\mathbf{\Omega}^2\} \quad V = \{\mathbf{S}^2\mathbf{\Omega}^2\} \tag{2.24}$$

For 2D mean flows, only  $I_{\mathbf{S}}$  and  $I_{\mathbf{\Omega}}$  are independent while  $III_{\mathbf{S}} = 0$ , IV = 0 and  $V = II_{\mathbf{S}}II_{\mathbf{\Omega}}/2$ . The EARSM-coefficients,  $\beta_i$ , can be derived in a number of different ways. Depending on the choice of basis tensors, an EARSM can be denoted complete or incomplete. A complete EARSM exactly solves the ARSM-equation (2.21) and is based on a complete set of basis tensors implying five or more basis tensors for the most general case since  $a_{ij}$  has five independent components. An incomplete EARSM is, correspondingly, based on an incomplete set of basis tensors and hence only provides an approximation to the solution to the (2.21). In common for all approaches is that  $\mathcal{P}/\varepsilon = -a_{ij}S_{ji}$  is

treated as a free parameter. In this way the scalar nonlinearity in  $a_{ij}$  is "overcome" initially but has to be adressed at a later stage. Complete EARSMs, the treatment of the dependency on  $\mathcal{P}/\varepsilon$  of the EARSM-coefficients as well as different derivation techniques for incomplete EARSMs will be further discussed in the following chapter.

Although, the dependency on the mean rotation rate tensor makes an EARSM sensitive to rotation and curvature effects, the underlying weak equilibrium assumption implying that the advection is neglected, may lead to rather poor predictions in flows where rotation and curvature effects are strong. By assuming weak equilibrium in a general curvi-linear coordinate system an additional term (curvature correction) on the form

$$-\tau(a_{ik}\Omega_{kj}^{(r)} - \Omega_{ik}^{(r)}a_{kj}) \tag{2.25}$$

arises on the left-hand side of the ARSM-equation (2.21) where  $\Omega_{ij}^{(r)}$  represents the the local rotation rate of the flow. This has been studied by, e.g., Sjögren (1997), Girimaji (1997), Wallin & Johansson (2002) and Gatski & Wallin (2004). The contribution (2.25) can be directly incorporated in an EARSM through the transformation  $\Omega_{ij} \to \Omega_{ij}^* = \Omega_{ij} - \tau \Omega_{ij}^{(r)}/A_0$  where  $A_0$  is a model parameter, if the modelling of (2.21) includes terms in  $\Omega_{ij}$  of tensorial order one or less.

In some generic flows subject to system rotation, the curvature correction (2.25) is exact and accounts for the complete advection. For this case the curvature correction is on the form

$$\Omega_{ij}^{(r)} = -\epsilon_{ijk}\omega_k^{(s)} \tag{2.26}$$

where  $\omega_k^{(s)}$  are the components of the system rotation rate vector. This yields a significant improvement in, for instance, rotating channel flow where mean velocity predictions in good agreement with DNS can be achieved, see Wallin & Johansson (2002). In other more complex flows where the exact expression for  $\omega_k^{(s)}$  cannot be found, the inclusion of the curvature correction can still improve the predictions significantly, see Hellsten  $et\ al.\ (2002)$ .

### 2.2.2.1. Eddy-viscosity based models

A family of models that is somewhat related to EARSMs, due to being explicit, is that of those based on the eddy-viscosity assumption. The eddy-viscosity type of closure arises naturally when assuming that the turbulent stresses can be modelled in terms of an extra viscous stress. This approach is based on the original Bousinessq hypothesis, Boussinesq (1877), which relates the shear component of the Reynolds stress in nearly parallel flows to the cross-stream mean velocity gradient. The generalization of this concept relates the Reynolds stress tensor directly to the mean strain rate tensor and yields a constitutive relation on the form

$$\overline{u_i'u_j'} = -2\nu_T S_{ij} + \frac{2}{3}K\delta_{ij} \tag{2.27}$$

The modelling problem is hence reduced to determining the eddy viscosity,  $\nu_T$ , which is of dimension [velocity]·[length]. The computationally cheapest method to do this is to choose a velocity scale based on the mean flow and a length scale related to the geometric properties of the problem. This is commonly referred to as an algebraic model and an example of this is the model proposed by Baldwin & Lomax (1978). However, the most common approach is to apply a two-equation platform mentioned earlier, implying that (2.15) and (2.17) are used in combination with (2.27). A natural choice for the velocity scale is hence the square root of the turbulence kinetic energy,  $\sqrt{K}$ , while the length-scale can be determined from the auxiliary quantity in combination with K. A two-equation model that has been used in numerous studies is the  $K-\omega$  model proposed by Wilcox (1988).

Once the velocity and length scales have been established the eddy viscosity can be determined through the relation

$$\nu_T = C_\mu \frac{K^2}{\varepsilon} \tag{2.28}$$

where  $C_{\mu}$  is a parameter.

One of the major drawbacks with models based on the standard eddy-viscosity assumption is their insensitivity to rotation. This means that the governing equations for the turbulence quantities take the same form in a rotating system of reference as in an inertial frame. Standard eddy-viscosity models therefore make poor predictions in many flows affected by streamline curvature and rotation. Even generic flows such as rotating channel and rotating pipe provide insurmountable challenges for this kind of closures. There have, however, been successful efforts of introducing sensitivity to rotation in eddy-viscosity models. Pettersson-Reif et al. (1999) introduced a dependency of  $\nu_T$  on the system rotation rate and the second invariant of the mean rotation rate tensor,  $\Pi_{\Omega}$ . In doing so Pettersson-Reif et al. (1999) showed that good agreement between RANS-computations and DNS can be obtained in 2D mean flows such as rotating channel.

#### 2.3. Generic test cases

In the present study, a number of generic flows are used to evaluate and analyse the performance of different modelling approaches. Common for all these flows is that the effects of system rotation and streamline curvature are strong. The most fundamental of these cases is rotating homogeneous shear flow. Homogeneous shear flow is a 2D mean flow in which the only nonzero mean strain tensor component(s) is  $S_{12}$  (and  $S_{21}$ ). This component is set to some prescribed value. From this point of view this case is rather special since the turbulence has no effect on the mean flow. The rotation is normally applied in the third direction orthogonal to the plane in which the shear is confined. Since this flow is homogeneous in space there is no spatial dependence on the averaged quantities. Therefore, in most investigations concerning (rotating) shear flow there is a focus on how different quantities evolve in time. The response of the

turbulence is strongly dependent on the magnitude and sign of the rotation, see for instance Bardina et al. (1983).

Another 2D mean flow considered is fully developed turbulent rotating channel flow. The geometry of the case is very simple with two parallel infinite walls. The flow between the walls is driven by a constant pressure gradient in the streamwise direction which together with the spanwise direction are treated as periodic directions for the fully developed case when direct numerical simulations are performed. The mean quantities are dependent on the wallnormal direction only why a RANS-closure is easily implemented in a numerical solver for 1D problems. In the present study, as in many previous studies, the rotation is applied in the spanwise direction. This divides the channel into one suction side and one pressure side. The applied system rotation rate has many interesting effects on the flow. For instance, the slope of the mean velocity profile in the center of the channel is approximately twice the system rotation rate. There is also a difference between the wall-shear velocities, defined as  $u_{\tau} =$  $\sqrt{\nu \frac{dU}{du}}|_{wall}$ , for the suction and pressure side of the channel. This difference intially increases for low rotation numbers and then decreases with increasing rotation number, see Alvelius (1999). Furthermore, for high rotation numbers the turbulence is strongly surpressed on the suction side of the channel. For further discussions regarding channel flow see chapter 4 and paper 5.

The only generic test case, in the present study, that constitutes a 3D mean flow is fully developed rotating pipe flow. This flow is obtained by letting a pressure gradient push fluid through an infinitely long cylindrical pipe which rotates around its axis of symmetry. This mean flow is three dimensional since the mean flow invariant  $V \neq II_{\mathbf{S}}II_{\mathbf{\Omega}}/2$ . The two most characteristic features of this flow are the parabolic-like mean azimuthal velocity profile and the increasing bulk flow for increasing rotation rate of the pipe for a constant pressure gradient. While the increased bulk flow can be captured with many RANS turbulence models, the deviation of the mean azimuthal velocity from solid body rotation is governed by an intricate balance, see Wallin & Johansson (2000), and provides a discriminating test case for any turbulence model. Previous studies have demonstrated that many RANS-closures tend to predict the wrong sign of the correlation between the azimuthal and axial velocity fluctuations, see for instance Pettersson et al. (1998) and Jakirlić et al. (2002) but also Grundestam et al. (2005). Rotating pipe flow is dependent on one spatial coordinate only and is therefore, as channel flow, suitable for implementation in a 1D solver. Different aspects of rotating pipe flow is further discussed in papers 1-3.

#### CHAPTER 3

# Formulation of EARSMs

A large part of the present study concerns explicit algebraic Reynolds stress models. Besides deriving and testing a new EARSM, different EARSM representation techniques based on incomplete sets of basis tensors are investigated. In this chapter, these and other aspects of the EARSM type of turbulence model are presented.

#### 3.1. Complete EARSMs

A complete EARSM is an explicit tensorially exact solution to the ARSM-equation (2.21). In all previous EARSM studies tensorially linear modelling has been used. The reason for this is easily understood - the system of equations governing the EARSM-coefficients,  $\beta_i$ , will contain nonlinearities if modelling nonlinear in  $a_{ij}$  is used. This implies that it will be impossible to find the corresponding solution on closed form for most cases. With respective to this, the modelling concerning EARSMs has in the present study been restricted to the quasi-linear form (2.19) presented in the preceding chapter. In what follows the strain and rotation rate tensors are assumed to be nondimensionalized with the turbulence time-scale,  $\tau$ .

Inserting (2.19) together with the expression for the production

$$\frac{\mathcal{P}}{\varepsilon} = -\frac{4}{3}\mathbf{S} - (\mathbf{a}\mathbf{S} + \mathbf{S}\mathbf{a}) + \mathbf{a}\mathbf{\Omega} - \mathbf{\Omega}\mathbf{a}$$
 (3.1)

in the ARSM-equation (2.21) yields the modelled ARSM-equation which can be written

$$N\mathbf{a} = -A_1\mathbf{S} + (\mathbf{a}\mathbf{\Omega} - \mathbf{\Omega}\mathbf{a}) - A_2(\mathbf{a}\mathbf{S} + \mathbf{S}\mathbf{a} - \frac{2}{3}\{\mathbf{a}\mathbf{S}\}\mathbf{I})$$
(3.2)

where  $N = A_3 + A_4 \mathcal{P}/\varepsilon$ . The parameters are related through the transformations

$$A_0 = \frac{C_4}{2} - 1 \quad A_1 = \frac{3C_2 - 4}{3A_0} \quad A_2 = \frac{C_3 - 2}{2A_0}$$

$$A_3 = \frac{2 - C_1^0}{2A_0} \quad A_4 = \frac{-C_1^1 - 2}{2A_0}$$
(3.3)

By assuming that N is a free parameter, an exact solution for the Reynolds stress anisotropy can be obtained by inserting a complete expansion (2.22) in (3.2) and solving for the  $\beta$ -coefficients. This has been done for 2D mean flows by Pope (1975) and general 3D mean flows and different underlying model

assumptions by, e.g., Taulbee (1992), Gatski & Speziale (1993) and Wallin & Johansson (2000). For three-dimensional mean flows the Reynolds stress anisotropy tensor has five independent components due to being symmetric and traceless. Therefore five independent basis tensors must be used, one for each degree of freedom. In some cases it may be convenient to express the EARSM in terms of more than five basis tensors, see for instance Gatski & Speziale (1993). However, any extra basis tensor chosen in addition to these five independet basis tensors can be expressed in terms of these five tensors if the coefficients are allowed to be rationals of polynomials of the mean velocity invariants (2.24), see Taulbee  $et\ al.\ (1994)$ . This can in some cases cause singularity problems, see Grundestam  $et\ al.\ (2005c)$  for a discussion regarding this in rotating pipe flow.

Since N has been treated as a free parameter, the scalar nonlinearity due to  $\mathcal{P}/\varepsilon$  must be dealt with after the EARSM-coefficients have been derived. The most simple way to address this problem is to let N attain a prescribed value. This approach was used by Gatski & Speziale (1993) where the corresponding assymptotic equilibrium value was used. Unfortunately, this method gives models that make poor predictions in flows with high shear rates. Wallin (2000) demonstrated that the corresponding EARSM gives the wrong assymptotic behaviour for large shear rates. This was also noted by Speziale & Xu (1996). A correct behaviour of N implies consistency between  $\mathcal{P}/\varepsilon$  evaluated from the anisotropy and strain rate tensors, and the explicit dependency of the EARSM coefficients on  $\mathcal{P}/\varepsilon$  through N. This can be achieved by solving the governing equation for N which is given by  $N = A_3 - A_4\{aS\}$  where the EARSM gives the expression for a. With the modelling used in (3.2), N is governed by a sixth order polynomial equation for three dimensional mean flows while the corresponding equation for two dimensional mean flows is of third order. Hence, the consistency condition can only be exactly fulfilled for two dimensional mean flows if N is to be evaluated from an explicit expression. EARSMs which fullfil this condition are usually referred to as self-consistent and have been derived independently by Girimaji (1996) and Johansson & Wallin (1996) for two dimensional mean flows. Wallin & Johansson (2000) proposed an approximation for 3D mean flows in terms of a correction to the 2D expression for N that have been shown to improve the predictions in rotating pipe flow significantly, see Wallin & Johansson (2000) and Grundestam et al. (2005).

## 3.2. Incomplete EARSMs

While a complete set of basis tensors yields the exact solution (in terms N) to the ARSM-equation, an incomplete set of basis tensors can be used to derive an approximate solution. The use of incomplete sets of basis tensors can be questioned since the corresponding EARSM will not provide a tensorially exact solution to the ARSM-equation. However, if a robust implementation of complete EARSM for 2D mean flows in a general CFD-code is assumed to exist, it is indeed motivated to investigate what an incomplete EARSM, based on the same set of basis tensors as the 2D formulation, derived for general 3D mean

flows can offer. In this way, a whole new model does not need to be reimplemented with all numerical problems this may cause. Instead, use of old routines can be made and the modifications to the code can be restricted to changing the evaluation of the EARSM coefficients. The use of incomplete EARSMs hence provides a systematic way of improving flow predictions of already existing codes without doing extensive reimplementations. From this perspective, approximate approaches are indeed very interesting since one can literally choose which basis tensors to include and which to leave out. This must, however, be done with care since the different basis tensors listed in (2.23) have different properties and hence the actual choice can have a significant effect on the performance of the EARSM.

The second aspect to consider is the derivation method. A method used by several authors for this purpose is based on the Galerkin method. This approach was first used to derive EARSMs by Jongen & Gatski (1998), but since then, several authors have applied this approximation procedure, see Rumsey et al. (2000), Rung (2000) and Manceau (2003). An alternative approach based on the least-squares method was recently proposed by Grundestam et al. (2005c). Below, these two methods will be compared and discussed.

The Galerkin method which is often used in finite element methods, can also be applied to the ARSM-equation to derive an EARSM. The system of equations governing the EARSM-coefficients is obtained by inserting the expansion of  $a_{ij}$  (2.22) in (3.2). Each and everyone of the basis tensors used in (2.22) is then multiplied from the left and the trace is formed. If the ij-th component of the ARSM equation is denoted  $ARSM_{ij}(\mathbf{a}, \mathbf{S}, \mathbf{\Omega}, N)$ , the Galerkin method gives, after applying the representation of  $\mathbf{a} = \beta_l \mathbf{T}^{(l)}$ , the system of equation governing the  $\beta_i$ -coefficients as

$$T_{ij}^{(k)}ARSM_{ij}(\beta_l \mathbf{T}^{(l)}, \mathbf{S}, \mathbf{\Omega}, N) = 0 \quad k = 1, \dots, M$$
 (3.4)

where M is the number of basis tensors. In addition to (3.4) an equation for N has to be solved. The Galerkin method yields an exact solution if a complete set of basis tensors is used. If  $A_2$  is zero or nonzero, two or three, respectively, basis tensors are needed solve (3.2) exactly for 2D mean flows, see Jongen & Gatski (1998) and Wallin & Johansson (2000). Commonly used basis tensors are  $\mathbf{T}^{(1)}$ ,  $\mathbf{T}^{(2)}$  and  $\mathbf{T}^{(4)}$ . In the study by Jongen & Gatski (1998), it was shown that a general (3D) EARSM based on these tensors is exact not only for 2D mean flows, but also for 3D mean flows in which one of the eigenvectors of  $\mathbf{S}$  is aligned with one eigenvector of  $\Omega$ .

In a recent study by Grundestam et al. (2005c), an alternative procedure for deriving EARSMs based on incomplete sets of basis tensors was proposed. The method is based on minimizing the error in the ARSM-equation due to using incomplete sets of basis tensors. Under the assumption that N is an independent parameter, a complete EARSM exactly satisfies the ARSM-equation. When an incomplete representation is used, the ARSM-equation cannot be exactly fulfilled and an error,  $E_{ij}$ , is induced. This error tensor has components

given by

$$E_{ij} = ARSM_{ij}(\beta_l \mathbf{T}^{(l)}, \mathbf{S}, \mathbf{\Omega}, N)$$
(3.5)

The minimization is done by considering the scalar square error,  $E_{ij}E_{ij}$  with respect to the EARSM-coefficients. The governing system of equations is obtained by differentiating the square error with respect to the different  $\beta_i$ -coefficients and setting each and everyone of the corresponding equations equal to zero. Hence, the system of equations is given by

$$\frac{\partial E_{ij}E_{ij}}{\partial \beta_{\nu}} = 0 \tag{3.6}$$

where k = 1, ..., M and M is the number of basis tensors.

Both the above methods provide ways of deriving incomplete EARSMs that should be expected to improve predictions compared to the corresponding 2D mean flow formulations when used in general 3D mean flows. The formal optimality characteristics are, however, somewhat intricate and are discussed below. It can be pointed out that the least-squares based procedure tends to give somewhat more algebraically complex EARSM-coefficients than the Galerkin method. This should, however, be of less importance since code generating and symbolic manipulation software such as MAPLE is available.

As an illustration of the differences in predictions between EARSMs based on the same set of basis tensors but derived with the two different techniques, fully developed turbulent rotating pipe flow can be studied. Rotating pipe flow constitutes, by definition, a three-dimensional mean flow that provides a discriminating test case for turbulence models. The mean flow predictions of four different EARSMs based on the same incomplete set of basis tensors are shown in figure 3.1 for rotation numbers  $Z = U_w/U_b = 0.5$  and 1 where  $U_w$  is the azimuthal velocity of the wall and  $U_b$  is the mean bulk velocity. The Reynolds number based on  $U_b$  and the pipe diameter, D, is  $Re = U_b D/\nu = 20000$ . The basis tensors used are  $\mathbf{T}^{(1)}$ ,  $\mathbf{T}^{(4)}$  and  $\mathbf{T}^{(5)}$ .

Two sets of model parameters in combination with the two different derivation procedures are considered. The EARSMs denoted G and LS are derived with the Galerkin and least-squares methods, respectively, and correspond to the same model parameter set as the curvature corrected WJ-EARSM proposed by Wallin & Johansson (2002) which implies  $A_2=0$ . The two other EARSMS, GA2 and LSA2, are also derived with the Galerkin and least-squares methods but have model-parameter sets corresponding to the L-SSG as given by Gatski & Speziale (1993). The predictions of the corresponding complete EARSMs, WJ-EARSM and L-SSG including the curvature correction with model parameters as given by Wallin & Johansson (2002), are also plotted in figure 3.1 together with the experimental data by Imao et al. (1996). The curvature correction proposed by Wallin & Johansson (2002) has been used in all computations.

From figure 3.1 it is clear that there is a significant difference in the prediction of the Galerkin and least-squares based EARSMs. What is even more

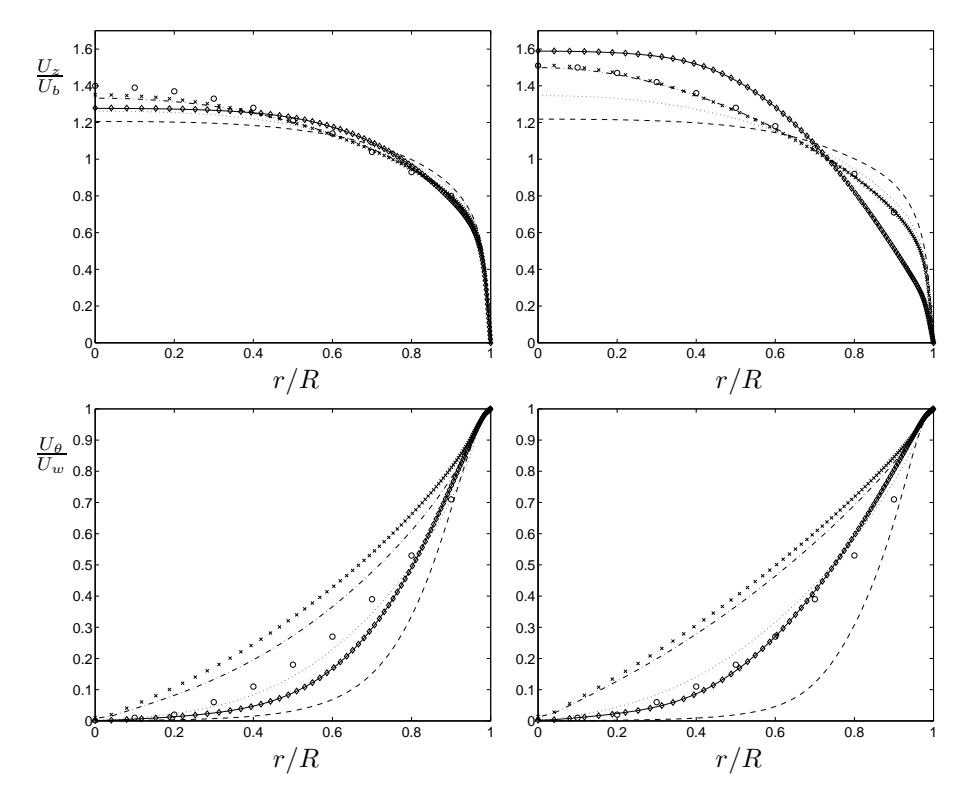


FIGURE 3.1. Normalized mean axial and azimuthal velocities,  $U_z/U_b$  (upper) and  $U_\theta/U_w$  (lower), for  $Z = U_w/U_b = 0.5$  (left) and 1.0 (right). LS (-), G (--), WJ-EARSM ( $\diamond$ ), LSA2 (-·), GA2 (···), L-SSG ( $\times$ ) and experiments ( $\diamond$ ) Imao *et al.* (1996).

important is that the least-squares EARSMs are in much better agreement with the complete EARSMs. The LS-EARSM is virtually indistinguishable from the WJ-EARSM in this perspective. The Galerkin EARSMs are more off and show little sensitivity to the increased rotation. It should, however, be pointed out that for a different set of model parameters and choice of basis tensors, the differences might not be as striking as in figure 3.1. In fact, in the study by Grundestam et al. (2005c) good agreement with the complete EARSM of the mean axial velocity profile was achieved with an EARSM based on  $\mathbf{T}^{(1)}$ ,  $\mathbf{T}^{(2)}$  and  $\mathbf{T}^{(4)}$  for the model parameters corresponding to the GA2 and LSA2 EARSMs.

## 3.2.1. Optimality

Whenever an approximation is derived or used, the accuracy and optimality of the approximation are natural and important aspects to investigate. This is also the case for EARSMs based on incomplete sets of basis tensors. Hands-on computations of a particular flow case can demonstrate how close the predictions of an incomplete EARSM are to those of the exact EARSM and hence provide some indication of the accuracy of the approximation. However, even though a particular incomplete EARSM gives good predictions in some flow(s), it is always reassuring to have understanding of the optimality aspects of the representation method.

The Galerkin method yields approximations that are optimal in a strict sense if the system matrix is symmetric and positive definite. In the context of EARSM representations, these issues can be studied by rewriting the ARSMequations as

$$A_{ijpq}a_{pq} = r_{ij} (3.7)$$

where

$$A_{ijpq} = -N\delta_{ip}\delta_{jq} + \delta_{ip}\Omega_{qj} - \delta_{jq}\Omega_{ip}$$

$$-A_{2}(\delta_{ip}S_{qj} + S_{ip}\delta_{qj} - \frac{2}{3}\delta_{ij}S_{pq})$$

$$r_{ij} = -A_{1}S_{ij}$$
(3.8)

$$r_{ij} = -A_1 S_{ij} (3.9)$$

 $a_{pq}$  is the Reynolds stress anisotropy. The necessary optimality conditions are symmetry  $(A_{ijpq} = A_{pqij})$  and positive definiteness  $(X_{ij}A_{ijpq}X_{pq} > 0$  for any tensor with components  $X_{ij}$ ). If these conditions are fulfilled the representation,  $a_{pq}^{rep}$ , is optimal in the sense that the error  $e_{ij} = a_{ij} - a_{ij}^{rep}$  is orthognal to  $a_{ij}^{rep}$  with respect to the inner product induced by  $A_{ijpq}$  given by  $(\mathbf{x}, \mathbf{y})_A = x_{ij} A_{ijpq} y_{pq}$ . Furthermore, the norm of the error,  $(\mathbf{e}, \mathbf{e})_A$  is minimal. Unfortunately, the terms of (3.8) that contain  $\Omega$  and  $\delta_{ij}S_{pq}$  are not symmetric and the eigenvalues of  $A_{ijpq}$  are not strictly positive. Therefore (3.8) is not symmetric nor positive definite. EARSMs derived with the Galerkin method in combination with the present choice of underlying modelling, are thus not optimal in this strict sense. See Grundestam et al. (2005c) for a detailed discussion of this. It is of course possible that Galerkin based EARSMs fulfill some other form of optimality criteria. Such optimality has not been shown in litterature though.

Important to note is that when the Galerkin method is used to represent a single tensor, the representation will be optimal in a least-squares sense. This is not in contradiction to the reasoning above since the system matrix for this case is given by the indentity matrix. It is crucial to keep these two fundamentally different cases distinguished in order to not falsely conclude that an optimal representation is achieved when the Galerkin method is applied to the ARSM-equation, as was done by Jongen & Gatski (1998).

EARSMs derived with the least-squares method are optimal in the sense that the error induced in the ARSM-equation is minimized in a square sense. From this perspective, the least-squares based EARSMs are on sound theoretical foundations since their optimality properties are known and of relevance.

Important to note is that even though the error in the ARSM-equation is minimized in a square sense when the least-squares method is applied, it

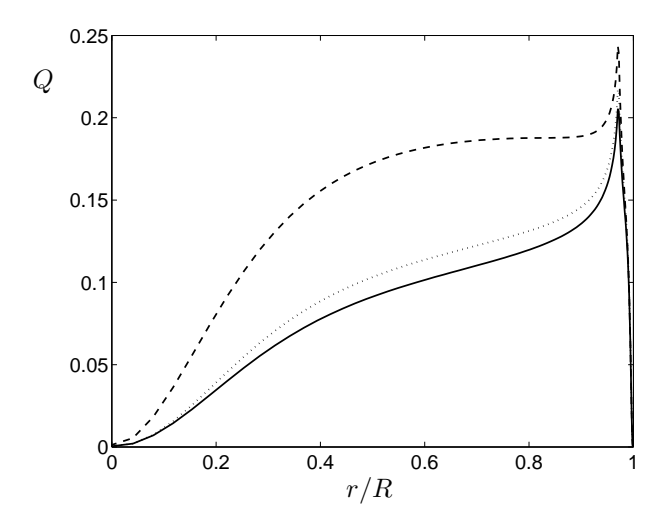


FIGURE 3.2. Square error for, Q, for GA2 (--), LSA2  $(\cdots)$  and MINA2 (-).

is not certain that the approximation of the anisotropy itself is more accurate with this method than with the Galerkin approach. It is therefore interesting to evaluate the square errors of the anisotropies computed with the corresponding EARSMs, respectively. For an incomplete representation ABC, the square error is given by

$$Q(ABC) = \sqrt{(a_{ij} - ABC_{ij})(a_{ij} - ABC_{ij})}$$
(3.10)

where  $a_{ij}$  denotes the corresponding complete EARSM. Evaluation of (3.10) has been performed for rotating pipe flow at Z=1 and Re=20000 using mean flow data from computations with the corresponding complete EARSM. In figure 3.2 the errors of GA2 and LSA2 are shown. In figure 3.2 a third type of EARSM, MINA2, is used as reference. This EARSM is based on the same set of basis tensors as GA2 and LSA2 and is optimal in the sense that Q(MINA2) is minimal, see Grundestam et al. (2005c) for details. As can be seen in figure 3.2, the error of LSA2 is significantly smaller than that of GA2. Furthermore, the difference between LSA2 and MINA2 is relatively small. It should be pointed out that the behaviour of the errors may be different in other types of flows and for other sets of basis tensors and model parameters.

# $3.2.2. \ Singularities$

The most significant deficit of using incomplete sets of basis tensor is singular behaviour. As discussed by for instance Grundestam  $et\ al.\ (2005c)$ , many incomplete EARSM representations are, in their full 3D mean flow form, singular for general or specific types of 2D mean flows such as strain and rotation free mean flows. This can be the case even though singular free 2D mean flow

formulations can be obtained from the 3D formulations by inserting the mean invariant properties for 2D mean flows,  $III_{\mathbf{S}} = 0$ , IV = 0 and  $V = II_{\mathbf{S}}II_{\mathbf{\Omega}}/2$ , and cancelling common factors in the denominator and numerator, see Grundestam et al. (2005c).

The application of a non-singular free EARSM can cause severe problems in general computational fluid dynamics (CFD) codes not only in cases where the fully developed flow fulfills some singularity criteria, but also when the flow is developing under the iterative process. Technically speaking, this singular behaviour can be ascribed to vanishing denominators of the EARSM coefficients under certain conditions. In most cases studied, one of the factors of the denominator is responsible for this and normally the same factor appears in the numerator in the limit of 2D mean flows. Mathematically this is hence a problem of zero-over-zero type. Therefore, if the reduction from general 3D mean flows to the problematic type of 2D mean flow(s) could be done algebraically in a CFD solver this type of singular behaviour could be dealt with. Implementing such an algorithm in a general CFD code might, however, not be worth the computational effort, especially if a singular free complete EARSM is available.

Singular behaviour could possibly occur even for complete EARSMs. The denominator of the EARSM proposed by Gatski & Speziale (1993) is rather complex and its behaviour in terms of singularity is not known. From this point of view the WJ-EARSM works very well. The 3D mean flow form has been proven to be non-singular for all types of flows including all 2D mean flows, see Wallin & Johansson (2002).

#### 3.3. Nonlinear modelling for EARSMs

Nonlinear modelling has previously been used in DRSMs in order to improve different aspects of a model. Speziale et al. (1991) incorporated a tensorially quadratic term in their pressure-strain rate model. Johansson & Hallbäck (1994) developed the most general expression for a rapid pressure strain rate model which of course included terms nonlinear in the Reynolds stress anisotropy tensor. This model was later used by Sjögren & Johansson (2000) in a DRSM which also incorporated nonlinear modelling of the slow pressure-strain and dissipation rate tensors. The DRSM by Sjögren & Johansson (2000) was constructed to satisfy realizability, see Lumley (1978), and was shown to give good predictions close to the wall without the use of wall-damping functions. In the study by Sjögren & Johansson (2000) terms tensorially nonlinear in the mean velocity gradients were also studied. These are on the form

$$\mathbf{N}^{\Omega} = -\frac{1}{\sqrt{-II_{\Omega}}} \left( \mathbf{a} \Omega^2 + \Omega^2 \mathbf{a} - \frac{2}{3} \{ \mathbf{a} \Omega^2 \} \mathbf{I} \right)$$
(3.11)

$$\mathbf{N}^{S} = \frac{1}{\sqrt{II_{\mathbf{S}}}} \left( \mathbf{a}\mathbf{S}^{2} + \mathbf{S}^{2}\mathbf{a} + \frac{2}{3} \{ \mathbf{a}\mathbf{S}^{2} \} \mathbf{I} \right)$$
(3.12)

assuming that S and  $\Omega$  are of dimension 1/time. Sjögren & Johansson (2000) demonstrated that (3.11) improved the predictions in a number of rotating flows. However, by including this additional term it is necessary to recalibrate the whole model. Since this is rather inconvenient, (3.12) can be included as well in order to give a zero net contribution of the terms in parallel flows if the same model parameter is used. Hence, there is no need for recalibration assuming that the original calibration was done for this type of flow.

While nonlinear modelling in terms of  $\bf a$  is easily incorporated in DRSMs, it seems virtually impossible to include such modelling in an EARSM due to the nonlinear nature of the system of equations governing the EARSM coefficients. From the EARSM perspective, the terms (3.11) and (3.12) are interesting since they are linear in  $\bf a$  and can therefore, at least in principle, be included directly. Such an investigation was performed by Grundestam et~al.~(2005) who proposed an EARSM incorporating a term nonlinear in the mean velocity gradients in the pressure-strain rate model. This model can be seen as a development of the EARSM proposed by Wallin & Johansson (2000) with a nonlinear extension of the rapid pressure-strain rate model.

One of the goals in the study by Grundestam et~al.~(2005) was to keep the EARSM coefficients as compact as possible and to use the same set of basis tensors as the parental model. Due to the excessive amounts of algebra generated with direct inclusion of (3.11) and (3.12), the nonlinear extension was on a slightly modified form compared to (3.11) and (3.12). The inclusion of the curvature correction, implies an ARSM-equation with a dependence on two different rotation rate tensors, the "standard" rotation rate tensor,  $\Omega$ , and the curvature corrected rotation rate tensor,  $\Omega^*$ . Whereas this can be dealt with algebraically by, for instance, using the representations presented by Grundestam et~al.~(2005), the corresponding EARSM would be very lengthy. Therefore, a more tractable procedure was sought for and  $\mathbf{N}^{\Omega}$  was reformulated in terms of  $\Omega^*$  as

$$\mathbf{N}_{approx}^{\Omega} = \frac{\sqrt{-II_{\Omega}}}{-II_{\Omega^*}} \left( \mathbf{a} \Omega^{*2} + \Omega^{*2} \mathbf{a} + \frac{2}{3} \{ \mathbf{a} \Omega^{*2} \} \mathbf{I} \right)$$
(3.13)

In the 2D mean flow limit (3.13) attains the same form as the original term (3.11) and is hence exact. For rotating pipe flow, it was shown by Grundestam et al. (2005) that (3.13) is relatively good approximation of (3.11) with a scalar error measure of the order 0.2. (3.12) was considered necessary to include in order to not have to recalibrate the whole model. Unfortunately,  $\mathbf{N}^S$  could not be conveniently expressed in terms of the cosen tensor basis and was therefore approximated with its 2D mean flow expression given by

$$\mathbf{N}_{2D}^S = \sqrt{II_{\mathbf{S}}}\mathbf{a} \tag{3.14}$$

The accuracy of (3.14) as an approximation of (3.12) is good in flows where the 3D mean flow effects are small. For rotating pipe flow, the error of (3.14) increases with increasing rotation rate of the pipe since the 3D mean flow effects become increasingly important, see Grundestam *et al.* (2005).

Applied to a number of generic test cases, the new EARSM makes interesting predictions. For the 2D mean flows rotating homogeneous shear flow and rotating channel flow, the nonlinear extensions give a good net contribution resulting in significantly improved overall model predictions. For rotating pipe flow the predictions were not all through improved. The nonlinear terms were, however, shown to have a significant effect on the predictions, see Grundestam et al. (2005). In the study by Grundestam et al. (2005) rotating pipe flow was studied and comparisons were made between the DRSM corresponding the new EARSM. The proposed EARSM has also been tested in a high-lift aeronatautics application, see Grundestam et al. (2005a), and was shown to give small but significant improvements of the predictions compared to the WJ-EARSM.

#### CHAPTER 4

# DNS of rotating channel flow

A direct numerical simulations (DNS) is a useful method for studying a particular flow in detail. In a DNS, the governing Navier-Stokes equations (2.2) are solved down to the smallest scales in space and time. This implies a tremendous computational effort in flows where there is a wide range of scales, i.e., at high Reynolds numbers. Therefore, DNS are restricted to more generic type of flows, such as channel flow, at limited Reynolds numbers. There are numerous DNS studies of channel flow, with and without system rotation, see for instance Kim et al. (1987), Moser et al. (1999), Kristoffersen & Andersson (1993), Lamballais et al. (1996) and Alvelius (1999). Orlandi & Fatica (1997) performed a simulations of turbulent rotating pipe flow.

In the present study, direct numerical simulations (DNS) of fully developed turbulent rotating channel flow at high rotation numbers have been performed. The computations were made using a pseudo-spectral code with fourier series expansions in the periodic streamwise and spanwise directions and Chebychev polynomials in the wall-normal direction. Simulations were performed for Reynolds number  $Re_{\tau} = u_{\tau}h/\nu = 180$  where  $u_{\tau}$  is the wall-shear velocity and h is the channel half-width. The computational domain was of size  $4\pi\delta \times 2\delta \times 2\pi\delta$  with a corresponding resolution of  $192 \times 129 \times 160$  in the streamwise, wall-normal and spanwise directions respectively. The system rotation was applied in the spanwise direction as in most previous studies including system rotation. The rotation numbers studied are  $Ro = 2h\Omega/U_b = 0.97, 1.07, 1.15, 1.21$  and 1.27 where  $U_b$  is the mean bulk velocity and  $\Omega$  is the spanwise system rotation rate.

The intention with this study is to investigate the flow physics at high rotation rates. Of special interest is the strong "Coriolis-force-stratification" of the flow in the wall normal direction and the behaviour of the wall-shear velocities on the stable and unstable side of the channel. The wall shear velocity is defined as  $u_{\tau} = \sqrt{\nu dU/dy}|_{wall}$  and the wall-shear velocities of the stable and unstable side are denoted  $u_{\tau}^s$  and  $u_{\tau}^u$ , respectively, and are related to the total wall-shear velocity through  $u_{\tau} = \sqrt{(u_{\tau}^{s2} + u_{\tau}^{u2})/2}$ . The aim is also to obtain a database with flow statistics that can be used for evaluation and testing of turbulence models.

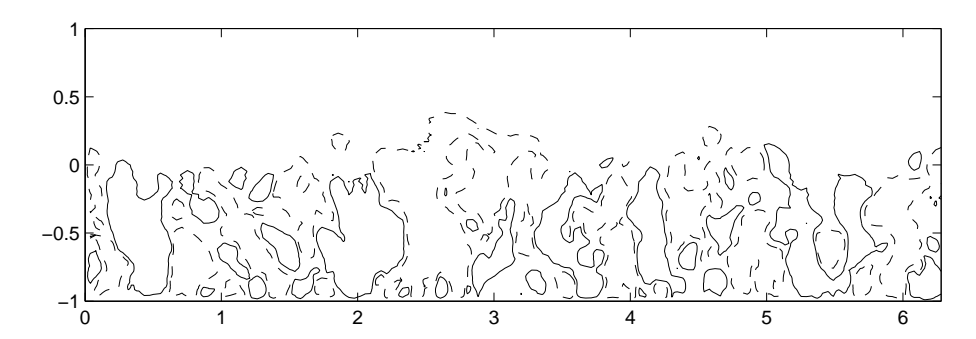


FIGURE 4.1. Contours of normalized wall-normal velocity,  $v'^+ = 1.0$  (-) and  $v'^+ = -1.0$  (--) in yz-plane for Ro = 1.27.

Rotating channel flow is governed by the Navier-Stokes equations formulated in a rotating frame of reference

$$\frac{\partial u_i}{\partial t} + u_j \frac{\partial u_i}{\partial x_j} = \frac{1}{\rho} \frac{\partial p^*}{\partial x_i} + \nu \frac{\partial^2 u_i}{\partial x_j \partial x_j} + 2\epsilon_{ijk} u_j \Omega_k \tag{4.1}$$

where  $u_i$  is the *i*th component of the instantenous velocity. Note that  $p^*$  in (4.1) denotes the reduced pressure given by  $p^* = p - \frac{\rho}{2}(\epsilon_{klm}\Omega_l x_m \epsilon_{kpq}\Omega_p x_q)$  in which the second part corresponds to the centrifugal force and p is the instantaneous pressure. The last term of (4.1) represents the Coriolis forces acting upon a fluid element. The centrifugal and Coriolis forces arise when the governing equations are transformed to a relative rotating coordinate system. A rotation axis in the spanwise direction implies  $\Omega_k = \Omega \delta_{k3}$  where  $\Omega$  is the system rotation rate.

The applied system rotation has a stratifying effect on the turbulence and divides the channel into one stable and one unstable side. Since the Coriolis force is proportional to the magnitude of the velocity, the force acting on particles close to the center of the channel is larger than the force on the particles closer to the wall. From (4.1) we see that the Coriolis force is pointing towards the side  $y/\delta < 0$ . Hence on this side, the high speed fluid particles in the center of the channel tend to change places with those closer to the wall. This leads to an increased mixing and therefore also higher turbulence levels on this side of the channel which is denoted the unstable side. On the stable side on the other hand, where the Coriolis force has the opposite effect, a decrease in the turbulence level is the result. This is illustrated in figure 4.1, in which contours of the wall-normal velocity are plotted for Ro = 1.27. Appearantly, the wall-normal velocity fluctuations are restricted to the unstable side. For a different set of rotation number and contour iso-value, the corresponding plot would of course look different from figure 4.1, not least since v' on the stable side decreases with increasing rotation rate. For all rotation numbers in the present study, there is, however, a clear restriction of v' to the unstable side of the channel.

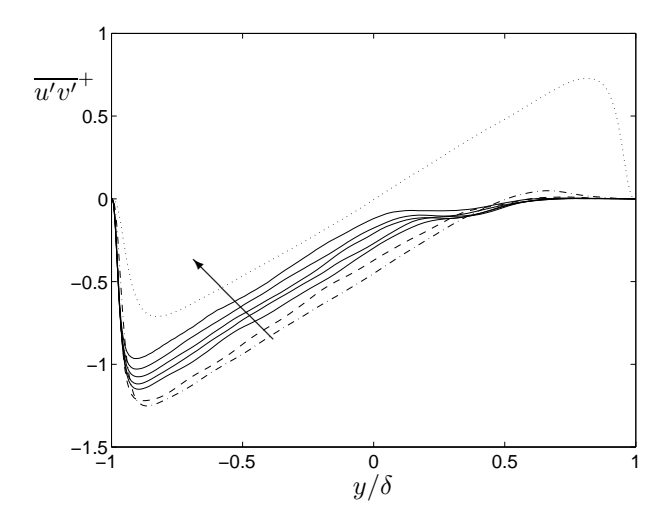


FIGURE 4.2. Normalized Reynolds shear stress,  $\overline{u'v'}^+$ . The arrow indicates increasing Ro for present the computations (-).  $(\cdots)$ ,  $(-\cdot)$  and (--) indicate Ro = 0, 0.43 and 0.77, respectively, from the simulations by Alvelius (1999).

Rotating channel flow is with its pure dependence on the system rotation suitable for studying the effect of rotation on turbulence. Rather interesting is the difference in behaviour of the statistical quantities. While the response of some quantities is monotonous with increased system rotation, e.g. the slope of the mean velocity profile in the center of the channel, other correlations show a nonmonotonous behaviour implying an increase or decrease until a certain threshold value of the rotation rate is reached after which the trend is shifted. An example of the latter is the normalized Reynolds shear stress,  $\overline{u'v'}^{\dagger}$ , shown in figure 4.2. The largest deviation from the nonrotating  $\overline{u'v'}^{\dagger}$ level is obtained for Ro = 0.43 among the different rotation numbers in the simulations by Alvelius (1999). For increasing rotation numbers above that value, the Reynolds shear stress is succesively shifted closer to the turbulent shear stress level of the nonrotating case on the unstable side of the channel. For the highest rotation number studied, Ro = 1.27, the  $\overline{u'v'}^+$ -profiles are rather close to each other in this region. In a large part of the stable side of the channel,  $\overline{u'v'}$  is very close to zero. This is a result of the very low wall-normal velocity fluctuations in this region discussed above and illustrated in figure 4.1.

The effect of the increased system rotation rate on the mean velocity behaviour is interesting not only because of the monotonous change of the slope of the mean velocity profile in the center of the channel, but also due to the nonmonotonous behaviour of the wall-shear velocities on the different sides of

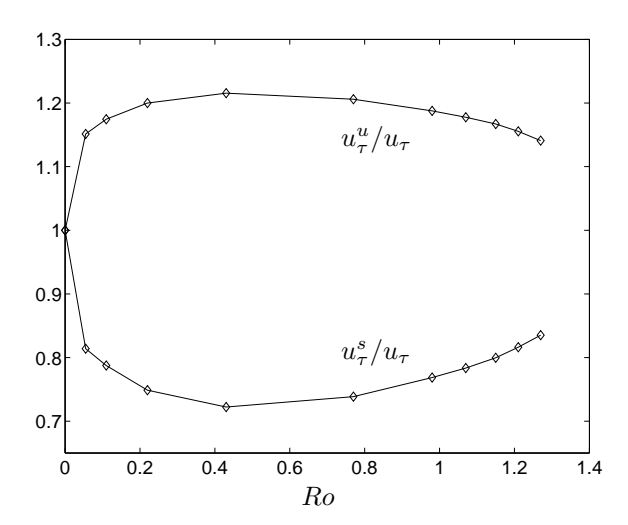


FIGURE 4.3. Wall-shear velocity ratio of the unstable,  $u_{\tau}^{u}/u_{\tau}$ , and stable side,  $u_{\tau}^{s}/u_{\tau}$ , side. DNS data for  $Ro \leq 0.77$  by Alvelius (1999).

the channel. In the center of the channel the slope of the mean velocity profile is close to  $2\Omega$  as noted earlier by, for instance, Kristoffersen & Andersson (1993) and Alvelius (1999). In the present study, this behaviour is confirmed but a small but significant deviation from this, with a trend towards a slightly smaller slope of the mean velocity, is observed, see paper 5. This also seems to be the case in the study by Alvelius (1999), at least for the higher rotation numbers. To present date, no strict proof has been given that dU/dy should equal  $2\Omega$  in the center of the channel. Oberlack (2001) has, by using symmetry methods, derived a scaling law dictating a direct proportionality dependence of dU/dy on  $\Omega$  in the center of the channel. This is a interesting result itself, but the actual proportionality coefficient is left as an undetermined parameter with this method.

Another interesting feature is the difference in wall-shear velocities between the stable and unstable side of the channel. As the rotation rate is increased from zero, the difference between  $u_{\tau}^s$  and  $u_{\tau}^u$  is increased until a certain rotation number is reached after which the difference decreases. This was noted in the study by Alvelius (1999) in which the threshold rotation number was Ro = 0.43. Comparisons made with the only higher rotation number, Ro = 0.77, indicated a decreasing difference between  $u_{\tau}^s$  and  $u_{\tau}^u$ . Alvelius (1999) further predicted that this was a trend that would hold also for higher rotation numbers. The present study does indeed confirm this and a plot showing  $u_{\tau}^s/u_{\tau}$  and  $u_{\tau}^u/u_{\tau}$  is given in figure 4.3. It should be noted that the difference for Ro = 1.27 in the present computations is actually smaller than for the case of lowest nonzero rotation number in the study of Alvelius (1999).

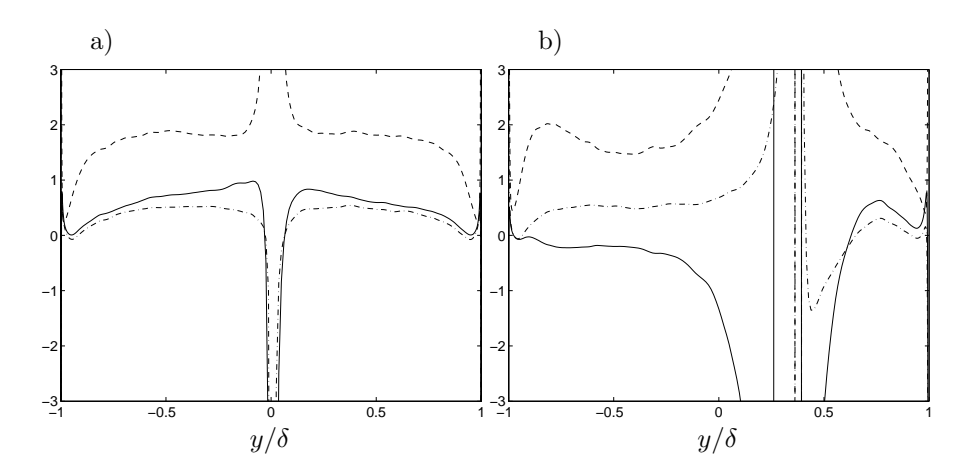


FIGURE 4.4. Ideal behaviour of the coefficients of the linear rapid pressure strain rate model for channel flow at  $Re_{\tau} = 360$  for a) Ro = 0.0 and b) Ro = 0.20.  $C_2$  (-·),  $C_3$  (--) and  $C_4$  (-).

#### 4.1. Least-squares optimizations of model parameters

The flow data obtained in a DNS can be used to evaluate the performance of turbulence models. This can be done not only by direct comparisons between the model predictions and the flow given by the DNS, but also by performing a priori tests of the different parts of a model. A priori tests of a number of different pressure-strain and dissipation rate models for rotating turbulent channel flow, based on the simulations by Alvelius (1999), are presented in paper 6. In the same paper, the ideal behaviour of the model coefficients for the rapid and slow pressure-strain and dissipation rate tensors are investigated. This is obtained by assuming a model representation on a particular tensorial form and then deriving the model coefficients that minimize the error in a least-square sense between that particular representation and the corresponding exact quantity. As an illustration of this, consider a model for the rapid pressure-strain rate tensor given by,

$$\tilde{\mathbf{\Pi}}^{(r)} = C_2 \mathbf{S} + \frac{C_3}{2} (\mathbf{a} \mathbf{\Omega} - \mathbf{\Omega} \mathbf{a}) - \frac{C_4}{2} (\mathbf{a} \mathbf{S} + \mathbf{S} \mathbf{a} - \frac{2}{3} \{\mathbf{a} \mathbf{S}\} \mathbf{I})$$
(4.2)

where the model parameters follow the notation of the more general expression (2.19). The minimization procedure used is the same as discussed in the preceding chapter. For this case the error to be minimized is given by  $\mathbf{E} = \tilde{\mathbf{\Pi}}^{(r)} - \mathbf{\Pi}^{(r)}$  where  $\mathbf{\Pi}^{(r)}$  is the exact rapid pressure strain rate tensor. The system of equations for the model coefficients  $C_i$  is given by  $\partial E_{ij} E_{ij} / \partial C_k = 0$  where k = 2, 3, 4. Hence, analytical expressions for  $C_k$  are obtained. These are, however, dependent on the exact tensor,  $\mathbf{\Pi}^{(r)}$ . Therefore, (4.2) cannot be used in a RANS-turbulence closure.

The final step involves inserting flow data from a particular DNS case into the respective expression and evaluate the results. The outcome of this exercise is shown in figure 4.4 a and b. The plots are based on the DNS-data obtained in the simulations by Alvelius (1999) of fully developed rotating turbulent channel flow for  $Re_{\tau}=360$  with Ro=0.0 and 0.20, respectively. For the particular case of channel flow, the representation (4.2) exactly matches the rapid pressure-strain rate tensor as given by the DNS. This is due to the fact that the tensor terms corresponding to  $C_2$ ,  $C_3$  and  $C_4$ , respectively, together form a complete basis since the rapid pressure-strain rate tensor has only three independent components for this particular case.

The behaviour of the C-coefficients reflects the well known fact that a linear model needs some sort of damping in the near-wall region in order to give accurate predictions. The radical behaviour in the center of the channel is due to the small mean velocity gradients there. This area is of less importance for the evaluations. For zero rotation, the  $C_2$  and  $C_3$  parameters are approximately constant in a region away from the wall. When rotation is applied  $C_2$  and  $C_3$ is more or less unaffected in this region.  $C_3$  gets a small positive bump close to the wall on the unstable side though. For zero rotation,  $C_4$  approximately follows a constant negative slope away from the wall. For the rotating case, the slope of  $C_4$  on the unstable side is increased and is approximately zero. For higher rotation numbers,  $C_2$  remains roughly the same on the unstable side of the channel while  $C_3$  and  $C_4$  tend to shift to higher levels and different slopes in this region, see paper 6. To be able to capture this behaviour over a wide range of rotation numbers provides a significant modelling challenge. Commonly used Van Driest type of damping approaches can be applied to the near-wall region. But in order to capture the shift of the original parameter that is seen for increasing rotation rates, more sophisticated modelling is needed.

#### CHAPTER 5

# Conclusions and outlook

The present study involves different aspects of Reynolds averaged Navier-Stokes turbulence modelling and direct numerical simulations of rotating channel flow. The modelling efforts are not directly focused on the development of a new supposedly optimal turbulence model. Instead, a number of issues, mainly related to EARSMs, are discussed. The flow cases used for testing and evaluation are, except for a high-lift aeronautics application, restricted to the generic flow cases of rotating turbulent channel and pipe flows.

The perhaps most directly applicable modelling result of this thesis is the EARSM based on a nonlinear pressure-strain rate model presented in paper 2. While this EARSM can be argued to be somewhat experimental, mostly due to the the somewhat ad-hoc formulation of the nonlinear extensions, it should still be considered as a realistic alternative in general CFD-codes. This is demonstrated in paper 4. in which the flow around a high-lift aeronautics application is computed. Comparisons show that the nonlinear contributions of the proposed EARSM give a positive effect on the predictions for many of the flow features compared to the parental WJ-EARSM. The perhaps most important aspect though, is the demonstration of functionality of the new EARSM in a general purpose flow solver for unstructured 3D grids. One of the drawbacks with the proposed EARSM is its possibility of being singular. This is the most serious deficit and could reduce the attraction of the model.

An important but less applied investigation, was undertaken in paper 1 in which incomplete EARSM representations were discussed. It was proven that incomplete EARSMs derived with the Galerkin method are not optimal in the least-squares sense argued by Jongen & Gatski (1998) and an alternative approach based on the minimization of the error in the ARSM-equation due to the use of incomplete sets of basis tensors, in a least-squares sense was proposed. Hands-on computations showed that the least-squares EARSMs performed radically better than the EARSMs derived with the Galerkin method. In all, from the more formal optimality perspectives as well as direct comparisons with the corresponding complete EARSM, this indicates that the least-square approach is better suited than the Galerkin method for deriving incomplete EARSMs. The most problematic feature of incomplete representations is singular behaviour. This normally occurs when a full 3D mean flow formulation is used for a general or a specific type of 2D mean flow. For some cases this type of singularity can be dealt with in a systematic way. This is, however, a problem

that has to be adequately adressed when an incomplete EARSM is used in a general 3D CFD solver.

The direct numerical simulation of fully developed rotating turbulent channel flow is perhaps more interesting both with respect to flow physics and modelling. The rotation numbers are rather high and the set of data obtained is a complement to the previous study by Alvelius (1999). The present numerical investigation also serves as a platform for future DNS investigations of the same flow case for other (higher) Reynolds and rotation numbers. Another related flow which might be of future interest is rotating Couette flow.

A future study would likely involve fundamental modelling aspects of the transport equations of the Reynolds stresses and the dissipation rate. From the modelling development point of view, the least-squares method provide an interesting approach. As was demonstrated in paper 6, it is possible to determine the ideal behaviour of some model parameters under certain circumstances. With respect to this, DNS data are very valuable for evaluating different parts of a turbulence model.

Whereas the velocity-scale in most turbulence closures is given by the equation for the turbulence kinetic energy, there is a wide spectrum of proposed quantities and corresponding equations for the length-scale. This is a research area where a priori testing can be applied, not only for the Reynolds stress transport equation but also for the dissipation rate equation. Detailed understanding of the different terms of dissipation rate equation would indeed assist the evaluation and development of any length-scale determining quantity and its transport equation.

#### CHAPTER 6

# Acknowledgement

First of all I wish to thank my supervisor Professor Arne Johansson for giving me the privilege of being his student. His guidance and knowledge in the field of turbulence have been invaluable during my doctoral studies. I also wish to my express my gratitude to Doctor Stefan Wallin for showing great interest in my work and for many interesting discussions. Stefan has greatly contributed to the outcome of this thesis.

A big thanks goes to Doctor Peter Eliasson at FOI for assisting with the EDGE-computations.

I have appreciated woorking in collaboration with my collegues in the HiAer project and I gratefully acknowledge the financial support from the European Union (Project Ref: G4RD-CT-2001-00448).

The mechanics department has provided a stimulating research environment with friendly people and an intellectual atmosphere. My room mates, present and former, deserve a special thanks. The contact with other people in our reseach group has been very important and is gratefully acknowledged. It has also been a pleasure to share thoughts and experiences with former doctoral students from the department.

I also wish to thank my friends outside the department. You are all very important to me. None of this would have been possible without good laughs and thrilling activities with you once in a while.

Finally, I want to thank my family for all the support and caring.

# **Bibliography**

- ALVELIUS, K. 1999 Studies of turbulence and its modelling through large eddy- and direct numerical simulation. PhD thesis, Department of mechanics, KTH, Stockholm, Sweden.
- Baldwin, B. & Lomax, H. 1978 This layer approximation and algebraic model for separated turbulence flow.  $AIAA\ Paper\ 78\text{-}257.$
- BARDINA, J., FERZIGER, J. H. & REYNOLDS, W. C. 1983 Improved turbulence models based on large-eddy simulation of homogeneous, incompressible turbulent flows. *Tech. Rep.*. Stanford University, tF-19.
- BOUSSINESQ, J. 1877 Essai sur la théorie des eaux courantes. *Mém. prés. Acad. Sci* 3rd edn, Paris XXIII, 46.
- Daly, B. J. & Harlow, F. H. 1970 Transport equations in turbulence. *Phys. Fluids* 13, 2634–2649.
- GATSKI, T. B. & SPEZIALE, C. G. 1993 On explicit algebraic stress models for complex turbulent flows. *J. Fluid Mech.* **254**, 59–78.
- Gatski, T. B. & Wallin, S. 2004 Extending the weak-equilibrium condition for algebraic reynolds stress models to rotating and curved flows. *J. Fluid Mech.* **518**, 147–155.
- GIRIMAJI, S., S. 1997 A galilean invariant explicit algebraic reynolds stress model for turbulent curved flows. *Phys. Fluids* **9**, 1067–1077.
- Girimaji, S. S. 1996 Fully-explicit and self-consistent algebraic reynolds stress model. Theor. and Comp. Fluid Dyn. 8, 387–402.
- GRUNDESTAM, O., WALLIN, S., ELIASSON, P. & JOHANSSON, A. V. 2005a Application of earsm turbulence model to high-lift aerodynamics applications. *Proc. of Engineering turbulence modelling and measurements (ETMM6)* Sardinia, Italy.
- Grundestam, O., Wallin, S. & Johansson, A. V. 2005b An explicit algebraic reynolds stress model based on a nonlinear pressure strain rate model. *Int. J. Heat Fluid Flow* **26**, 732–745.
- GRUNDESTAM, O., WALLIN, S. & JOHANSSON, A. V. 2005c Techniques for deriving explicit algebraic reynolds stress model based on incomplete sets of basis tensors and predictions of fully developed rotating pipe flow. *Phys. Fluids* 17.
- Grundestam, O., Wallin, S. & Johansson, A. V. 2006 Observations on the predictions of fully developed rotating pipe flow using differential and explicit algebraic reynolds stress models. *Euro. J. Mech. B/Fluids*.
- Hallbäck, M., Johansson, A. V. & Burden, A. D. 1996 The basics of turbulence

- $modelling.\ Chapter\ 3$  of Turbulence and Transition modelling. Kluwer Academic Publishers, iSBN 0-7923-4060-4.
- Hellsten, A., Wallin, S. & Laine, S. 2002 Scrutinizing curvature corrections for algebraic reynolds stress models. *In proc. of 32nd AIAA Fluid Dynamics Conference*.
- IMAO, S., ITOH, M. & HARADA, T. 1996 Turbulent characteristics of the flow in an axially rotating pipe. *Int. J. Heat Fluid Flow* 17, 444–451.
- Jakirlić, S., Hanjalić, K. & Tropea, C. 2002 Modeling rotating and swirling turbulent flows: A perpetual challenge. AIAA J. 40, 1984–1996.
- Johansson, A. V. & Hallbäck, M. 1994 Modelling of rapid pressure-strain in reynolds-stress closures. *J. Fluid Mech.* **269**, 143–168.
- JOHANSSON, A. V. & WALLIN, S. 1996 A new explicit algebraic reynolds stress model. Proc. sixth European Turbulence Conference pp. 31–34, lausanne, July 1996, Ed. P Monkewitz.
- Jongen, T. & Gatski, T. B. 1998 General explicit algebraic stress relations and best approximation for three-dimensional flows. *Int. J. Engineering Science* **36**, 739–763.
- Kim, J., Moin, P. & Moser, R. 1987 Turbulence statistics in fully developed channel flow at low reynolds number. *J. Fluid Mech.* **177**, 133–166.
- Kristoffersen, R. & Andersson, H. I. 1993 Direct simulations of low-reynoldsnumber turbulent flow in a rotating channel. *J. Fluid Mech.* **256**, 163–197.
- Lamballais, E., Lesieur, M. & Métais, O. 1996 Effects of spanwise rotation on the vorticity stretching in transitional and turbulent channel flow. *Int. J. Heat and Fluid Flow* 17, 324–332.
- Launder, B. E., Reece, G. & Rodi, W. 1975 Progress in the development of reynolds-stress turbulence closure. *J. Fluid Mech.* 41, 537–566.
- Lumley, J. L. 1978 Computational modeling of turbulent flows. Adv. Appl. Mech. 18, 123.
- Manceau, R. 2003 Accounting for wall-induced reynolds stress anisotropy in explicit algebraic stress models. In *Proceedings of the third international symposium on turbulent and shear flow phenomena*. Sendai, Japan.
- Moser, R. D., Kim, J. & Mansour, N. N. 1999 Direct numerical simulatio of turbulent channel flow up to  $re_{\tau}=590$ . Phys. Fluids 11, 943–945.
- OBERLACK, M. 2001 A unified approach for symmetries in plane parallel turbulent shear flows. *J. Fluid Mech.* **427**, 299–328.
- Orlandi, P. & Fatica, M. 1997 Direct simulations of turbulent flow in a pipe rotating about its axis. *J. Fluid Mech.*  $\bf 343$ , 43–72.
- Perot, B. & Natu, S. 2004 A model for the dissipation rate tensor in inhomogeneous and anisotropic turbulence. *Phys. Fluids* **16**, 4053–4065.
- Pettersson, B. A., Andersson, H. I. & Brunvoll, A. S. 1998 Modeling near-wall effects in axially rotating pipe flow by elliptic relaxation. *AIAA J.* **36**, 1164–1170.
- Pettersson-Reif, B. A., Durbin, P. & Ooi, A. 1999 Modelling rotational effects in eddy-viscosity closures. *Int. J. Heat Fluid Flow* **20**, 563–573.
- Pope, S. B. 1975 A more general effective-viscosity hypothesis. *J. Fluid Mech.* **72**, 331–340.
- Rodi, W. 1976 A new algebraic relation for calculating the reynolds stresses. Z. Angew. Math. Mech.  ${\bf 56},\,219-221.$

- Rumsey, C. L., Gatski, T. B. & Morrison, J. H. 2000 Turbulence model predictions of srongly curved flow in a u-duct. AIAA J. 8, 1394–1402.
- Rung, T. 2000 Entwicklung anisotroper wirbelzähigkeitsbeziehungen mit hilfe von projektionstechniken. PhD thesis, Technical University Berlin.
- SJÖGREN, T. 1997 Development and validation of turbulence models through experiment and computation. PhD thesis, Dept. of Mechanics, KTH, Stockholm, Sweden.
- SJÖGREN, T. & JOHANSSON, A. V. 2000 Development and calibration of algebraic nonlinear models for terms in the reynolds stress transport equations. *Phys. Fluids* 12, 1554–1572.
- Speziale, C. G., Sarkar, S. & Gatski, T. B. 1991 Modelling the pressure-strain correlation of turbulence: an invariant dynamical systems approach. *J. Fluid Mech.* 227, 245–272.
- SPEZIALE, C. G. & Xu, X. H. 1996 Towards development of second-order closure models for nonequilibrium turbulent flows. Int. J. Heat and Fluid Flow 17, 238– 244.
- Taulbee, D. B. 1992 An improved algebraic Reynolds stress model and corresponding nonlinear stress model. *Phys. Fluids* **A4**, 2555–2561.
- Taulbee, D. B., Sonnenmeier, J. R. & Wall, K. M. 1994 Stress relation for three-dimensional turbulent flows. *Phys. Fluids* **6**, 1399–1401.
- Wallin, S. 2000 Engineering turbulence modelling for cfd with a focus on explicit algebraic reynolds stress models. PhD thesis, Dept. of Mechanics, KTH, Stockholm, Sweden.
- Wallin, S. & Johansson, A. V. 2000 An explicit algebraic reynolds stress model for incompressible and compressible turbulent flows. J. Fluid Mech. 403, 89–132.
- Wallin, S. & Johansson, A. V. 2002 Modelling streamline curvature effects in explicit algebraic reynolds stress turbulence models. *Int. J. Heat and Fluid Flow* 23, 721–730.
- Wilcox, D. C. 1988 Reassessment of the scale-determining equation for advanced turbulence models. AIAA J. 26, 1299–1310.